Phys. Status Solidi RRL **6**, No. 2, 62–64 (2012) / **DOI** 10.1002/pssr.201105442

pss +++rapid research letters+++
www.pss-rapid.com

Experimental characterization of temperature-dependent electron transport in single-wall multi-tube carbon nanotube transistors

Paulius Sakalas[*,1,2], Martin Claus[,1], Michael Schroter[3,4], and Andrej Rumiantsev[5]**

[1] CEDIC, IEE, Technische Universität Dresden, Mommsenstr. 13, 01062 Dresden, Germany
[2] FRL, Semiconductor Physics Institute, Center for Physical Sciences and Technology, Goštauto 11, 01108 Vilnius, Lithuania
[3] RF Nano Corporation, 4311 Jamboree Rd. Suite 150, Newport Beach, CA 92660, USA
[4] UC San Diego, La Jolla, CA 92093, USA
[5] Cascade Microtech GmbH, Suss-Straße 1, 01561 Sacka, Germany

Received 20 September 2011, revised 25 November 2011, accepted 25 November 2011
Published online 1 December 2011

Keywords carbon nanotubes, transistors, optical phonons, phonon scattering, current gain, noise

[*] Corresponding author: e-mail sakalas@iee.et.tu-dresden.de, Phone: +49 351 46331910, Fax: +49 351 46337260
[**] e-mail Martin.Claus@tu-dresden.de, Phone: +49 351 46333053, Fax: +49 351 46337260

Current–voltage, radio-frequency (RF) and noise characteristics of single-wall multi-tube carbon nanotube (CNT) transistors were measured at cryogenic temperatures. Compared to an ambient temperature (T_a) of 300 K, only a slight drain current increase at $T_a = 77$ K was observed. In addition, a weak dependence of the maximum value of the current gain cut-off frequency (f_T) on T_a was obtained, indicating that f_T is rather limited by the device intrinsic quantum and extrinsic capacitances than by an improved mobility due to reduced optical phonon scattering at low T_a. A noise analysis of the devices at $T_a = 10$ K reveals that the noise factor (NF) improvement at very low temperatures is related to the reduced Nyquist noise of all resistive transistor noise contributors. Since the main noise source in CNTFETs is the shot noise, NF remains comparatively high even at $T_a = 10$ K.

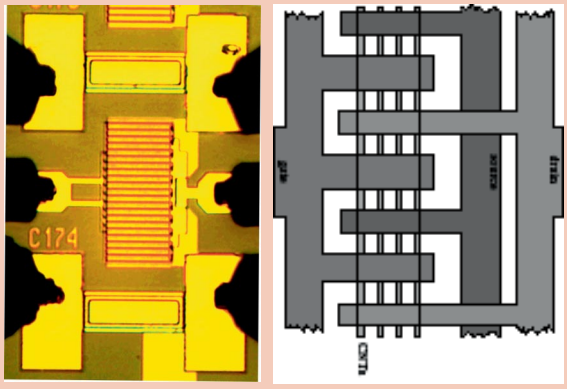

Photo of the CNTFET embedded in RF pads (left) and schematic layout of the CNTFET (right).

1 Introduction The high interest in using carbon nanotube (CNT) field-effect transistors (CNTFETs) in advanced electronics is based on their unique 1D transport properties resulting in quasi-ballistic transport, Coulomb blockade, Luttinger liquid behavior, and high linearity [1, 2]. The high carrier velocity together with the quasi 1D tube geometry yield theoretically and experimentally a very low intrinsic (quantum) capacitance per tube of $C_{QST} \sim 60$ aF/μm [3] giving a cut-off frequency f_T beyond 110 GHz μm in the ballistic limit [4]. The RF behavior of CNTFETs with thousands of tubes in parallel is not sensitive to tube diameter variations and the presence of metallic tubes in the channel [4]. Along with higher f_T, f_{max} and lower power dissipation compared to graphene FETs [4], CNTFETs are very attractive devices for analog high frequency applications. Electron scattering has been studied extensively for metallic tubes [5, 6] but less for semiconducting tubes: defects, physical bends, acoustic-phonon scattering at low bias and zone boundary optical phonon scattering at high bias [5]. The doping-free fabrication

procedure prevents from carrier freeze-out in CNTs and broadens the possible application area to ambient temperatures (T_a) starting from deep cryogenic temperature up to 573 K [8]. The investigation of CNTFETs at cryogenic temperatures enables a deeper understanding of CNT transport properties to provide insights for improving the device models [7] and the application-oriented device behavior.

In this work, DC, RF characteristics and the high-frequency noise factor of manufacturable top-gated multi-tube multi-finger CNTFETs were measured on wafer at room and cryogenic temperatures.

2 Device under test (DUT) Using a regular stepper-process and CVD growth of the CNTs, the CNTFETs can be placed deliberately anywhere on a wafer (manufacturable), thus enabling the fabrication of integrated analog circuits. The investigated high current CNTFETs typically have a few thousand CNTs in parallel directly connecting source and drain (no thin-film transistor) and were fabricated at RF Nano Corporation. Structures consist of a multi-tube and multi-finger layout with a fixed top gate length of 0.45 µm, a gate width of 40 µm, and 20 gate fingers. The source–drain spacing (channel length) is 800 nm. The devices were fabricated with the process technology described in Refs. [9–11]. To enable high frequency measurements the CNTFETs were embedded in RF pads, as it is seen in the left image of the abstract. The pad parasitics were de-embedded from the DUT *S*-parameters using "open" and "short" structures. On-wafer DC and AC (frequency range 0.1–10.5 GHz) standard characteristics were measured with a PNA 8361C at 300 K, 77 K and 10 K. The cryogenic measurements were carried out using Cascade Microtech PLC50 probe station, featuring temperature control within 0.5 °C and stability.

3 DC, RF and noise cryogenic performance Transfer characteristics at T_a = 300 K, 77 K and 10 K are shown in Fig. 1a. Due to the coexistence of metallic tubes (MT), the drain current I_d does not turn off at V_{gs} = –2.2 V. However, this is acceptable for RF applications as long as the intrinsic voltage gain is sufficiently above unity [12].

The drain current increase (~20%) at T_a = 77 K is not very significant compared to 300 K (Fig. 1). However, since acoustic-phonon and zone boundary optical phonon scattering has small impact on the DC current [13, 14] no clear conclusion regarding the temperature dependence of scattering can be drawn from the DC data. At T_a = 10 K a decrease of I_d is observed which is difficult to explain. In addition, a temperature dependent gate leakage current due to the temperature dependent mobility in HfO_2 [15] and a threshold voltage shift are observed. The threshold shift can also be observed in the transconductance g_m shown in Fig. 2a. This figure also shows only a slight increase of peak g_m with decreasing T_a up to 77 K. The output characteristics at T_a = 10 K, 77 K and 300 K at V_{gs} = –2 V, –1.5 V and –1 V are given in Fig. 1b. The maximum value of extrinsic low-field output conductance g_{ds} increases with decreasing T_a up to 77 K and then drops again with a further decrease of V_{ds}, see Fig. 2b. Such g_{ds} increase with decreasing T_a contradicts the observed conductance dependence on T_a of metallic single-wall CNTs which exhibit a linear increase of the conductance with increasing T_a [6].

However, for multi-tube CNTFETs the temperature dependence of the conductance may be complicated due to the coexistence of thousands MTs (we estimate that 1/3 of total CNTs are MTs) and semiconducting tubes (ST) in parallel, sometimes crossing each other [16] and bending back towards the contact stripes. ST crossed by MT suffers from an additional Schottky barrier formation [16]. Due to possible interaction between the crossed ST in CNTFETs the transport mechanism might be different from the single tube FET resulting in a different temperature dependence of the conductance. An important application related figure of merit (FoM) is the intrinsic voltage gain g_m/g_{ds}, which is larger than one for the investigated CNTFETs and highlights the capability of power amplification. The transducer

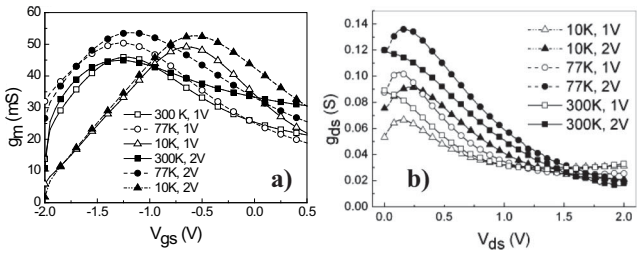

Figure 2 a) Extrinsic transconductance g_m versus V_{gs} at different T_a and V_{ds}; b) output conductance g_{ds} versus V_{ds}.

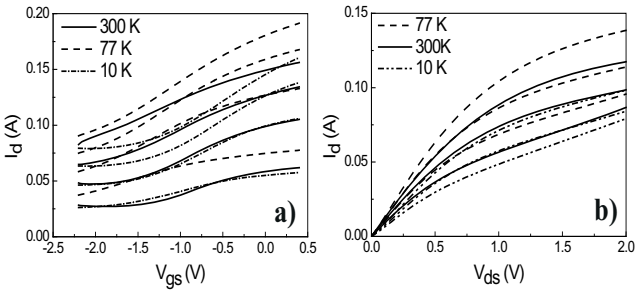

Figure 1 a) I_d versus V_{gs}. I_d increases with V_{ds} (V_{ds} = 0.5, 1, 1.5, 2 V). b) I_d versus V_{ds}. I_d increases with V_{gs} (V_{gs} = –2, –1.5, –1 V).

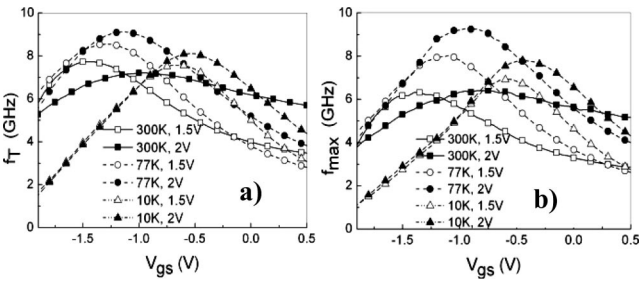

Figure 3 a) Current gain cut-off frequency f_T and b) maximum oscillation frequency f_{max} versus V_{gs}.

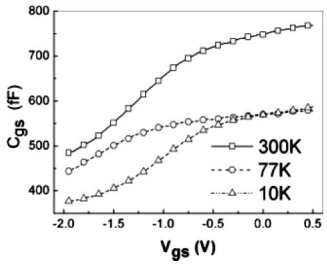

Figure 4 Gate–source capacitance C_{gs} versus V_{gs} at $V_{ds} = 0$ V.

power gain $G_T = 15$ dB at 1 GHz was obtained in matched load conditions. In contrast to graphene sheet FETs, where this ratio is much lower than "one" [12], for CNTFETs maximum values of $g_m/g_{ds} = 1.53$ (at 300 K, $V_{ds} = 1.5$ V, $V_{gs} = -1$ V), 2.9 (at 77 K, $V_{ds} = 1.9$ V, $V_{gs} = -1.2$ V), and 2.34 (at 10 K, $V_{ds} = 1.5$ V, $V_{gs} = -0.4$ V) were measured. This FoM shows the potential of CNT based technology for analog power applications operating in an extreme temperature environment. The peak value of the current gain cut-off frequency at 300 K is $f_T = 8$ GHz (pad de-embedded only, i.e. the contact finger structure remains) as shown in Fig. 3a. At $T_a = 77$ K f_T increases to 9 GHz only partially due to a transconductance increase (Fig. 2a). The bias and temperature dependence of the maximum oscillation frequency is given in Fig. 3b. Its minor temperature dependence seems to confirm that the contact resistance between the electrodes and CNTs does not vary with temperature down to at least 10 K [8]. Another contributor limiting f_T and f_{max} is the mobile tube charge and associated gate/source capacitance C_{gs}, which is also T_a dependent, see Fig. 4. The temperature dependence of C_{gs} may be explained with the T_a dependence of optical phonon scattering [13, 14]. At $T_a = 10$ K and at low bias, C_{gs} appears to be lower than that at 300 K. However, this is caused by a threshold voltage shift which was also visible in g_m. Generally, scattering increases the charge stored on the tube.

Assuming the reduction of scattering towards lower temperatures, the stored charge and associated capacitance then is expected to decrease with T_a as observed in Fig. 4. The noise factor in a 50 Ω environment was measured at different temperatures, Fig. 5a. NF in the frequency range of 1 to 3 GHz exhibits an improvement with decreasing T_a. Compared to SiGe HBTs which show 10 times lower NF at $T_a = 10$ K, CNTFETs exhibit only a slight NF improvement, which is due to their high shot noise contribution [17]. Noise analysis shows that the NF improvement at 10 K is partially due to the thermal noise reduction in the gate (R_g) and source (R_s) resistances. A minimum noise figure of NF_{min}(1 GHz, 300 K) = 3.5 dB with an associated gain of $G_{ass} = 12$ dB was obtained for the selected same CNTFET technology [17]. In this paper the investigated device exhibited NF_{min}(1 GHz, 300 K) = 4 dB in matched conditions (cf. Fig. 5a, open stars), which is about a factor of six smaller than NF. A rough estimate of NF_{min} at 10 K is about 1 dB. The associated gain is given in Fig. 5b. The NF improvement at $T_a = 77$ K is also related to higher RF gain: G_{ass}(77 K, 1 GHz) = 7.5 dB and G_{ass}(300 K, 1 GHz) = 5.8 dB.

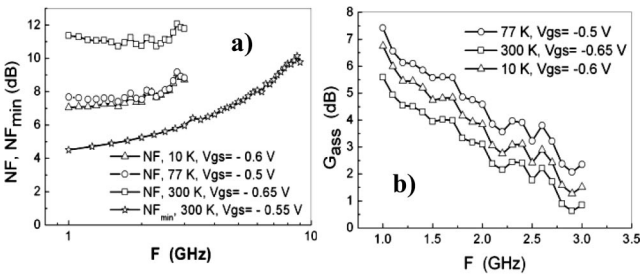

Figure 5 a) Noise factor NF and minimum noise figure NF_{min}. b) G_{ass} versus frequency at $V_{ds} = 1.9$ V.

4 Conclusions Since scattering has little impact on the DC characteristics, the channels can be long while maintaining the device linearity given by the transconductance. Slight increase of f_T at cryogenic temperatures is more related to the reduced C_{gs} rather than to the mobility as predicted in [13, 14]. Smaller NF at cryogenic T_a is obtained due to Nyquist noise reduction, but still NF remains high due to shot noise.

Acknowledgements F.-M. Werner, S. Giessmann, and A. Jachmann from Cascade Microtech are acknowledged for the support with cryogenic measurements.

References

[1] M. Bockrath et al., Nature **397**, 598–601 (1999).
[2] R. Egger and A. Gogolin, Phys. Rev. Lett. **79**(23), 5082–5085 (1997).
[3] D. Akinwande et al., IEEE Trans. Nanotechnol. **8**(1), 31–36 (2009).
[4] S.-O. Koswatta et al., IEEE Trans. Microw. Theory Tech. **59**(10), 2739–2750 (2011).
[5] Z. Yao et al., Phys. Rev. Lett. **84**(13), 2941–2944 (2000).
[6] H. W. Ch. Postma et al., Science **293**, 76–79 (2001).
[7] M. Claus, Ph.D. thesis, Technische Universität Dresden, TUD Press, ISBN 978-3942710237 (2011).
[8] T. Pei et al., Adv. Funct. Mater. **21**, 1843–1849 (2011).
[9] M. Schroter et al., Proc. Government Microcircuit Applications & Critical Technology Conference (GOMACTech), Orlando, FL, March 2011, pp. 367–370.
[10] M. Schroter et al., Proc. IEEE MTT-S International Microwave Symposium (IMS), ISBN 978-1-61284-757-3 (2011).
[11] M. Eron et al., Electron. Lett. **47**(4), 265–266 (2011).
[12] F. Ellinger et al., IEEE Int. Microwave and Optoelectronics Conf. (IMOC), Natal, Brazil, Oct./Nov. 2011, pp. 347–351.
[13] Y. Yoon et al., IEEE Trans. Electron Devices **53**(10), 2467–2470 (2006).
[14] J. Guo and M. Lundstrom, Appl. Phys. Lett. **86**, 193103 (2005).
[15] W. J. Zhu and T. P. Ma, IEEE Electron Device Lett. **25**(2), 89–91 (2004).
[16] M. S. Fuhrer et al., Science **298**, 494–497 (2000).
[17] P. Sakalas et al., Proc. Int. Conf. on Noise and Fluctuations (ICNF), Toronto, Canada, IEEE Conf. Proc. Catalog no. CFP1192N-CDR, ISBN 978-1-4577-0191-7 (2011).

